1000–1200 cm^{-1}, clearly are indicative of bidentate bridging sulfate groups.[15] The fine structure occurring at wavenumbers less than 750 cm^{-1} is unassigned. The bands undoubtedly include a variety of metal–oxygen modes.

The visible spectrum of I, Figure 3, was obtained from a pressed potassium bromide pellet at 77 K. This spectrum is one of the few available for solid-state plutonium compounds. Comparison of the visible spectrum of I with that of $Pu(SO_4)_2{\cdot}4H_2O$[16] does show a remarkable amount of similarity. In particular, the bands between 600 and 700 nm are very similar in shape and relative intensity in both cases. Peaks occurring at higher energies for both compounds are very abundant. The spectra are qualitatively similar although the resolution of the visible spectrum for I is significantly better.

The near-infrared spectrum of I, Figure 4, was obtained from a pressed potassium bromide pellet at 4 K. To the best of our knowledge this is the first report of the near-infrared spectrum for a hydrolyzed Pu(IV) compound in the solid state. Analysis of this spectrum will be attempted at a future date.

Acknowledgment. We wish to thank Dr. Lester R. Morss for his invaluable assistance in obtaining the thermogravimetric analysis. Special thanks are extended to Professor James A. Fahey for his help with the refinement of the cell constants.

Registry No. I, 82444-36-8.

---

(16) Leontovich, A. M. *Opt. Spektrosk.* **1957**, *2*, 695.

Contribution from the Department of Inorganic Chemistry,
University of Oxford, Oxford OX1 3QR, England

Oxygen Atom Transfer in Low-Temperature Matrices. 1. Formation and Characterization of Matrix-Isolated OMF_3 (M = P, As)[1a]

ANTHONY J. DOWNS,* GEOFFREY P. GASKILL,[1b] and SIMON B. SAVILLE

Received November 10, 1981

Ultraviolet photolysis of ozone isolated in a noble-gas matrix in the presence of the trifluoride MF_3 (M = P, As) results in the formation of the corresponding trifluoride oxide, OMF_3. The intensities and frequencies of the infrared absorptions due to the ^{16}O- and ^{18}O-substituted versions of the hitherto unknown molecule $OAsF_3$ are consistent with the expected C_{3v} symmetry. The vibrational spectra have been analyzed for information about the bonding in $OAsF_3$, and an attempt has been made to estimate the bond angles on the basis of the intensities in infrared absorption of the bond-stretching fundamentals.

Introduction

Although trifluoramine oxide[2] and the phosphorus trihalide oxides, OPX_3 (X = F, Cl, Br),[3] are well-characterized, surprisingly little is known about the analogous compounds of arsenic, antimony, and bismuth. It is quite possible that the formation of these compounds, like that of perbromates,[4] is hampered as much by kinetic as by thermodynamic barriers. It is also possible that the discrete molecular species characteristic, for example, of the phosphorus trihalide oxides[3] give place in the corresponding derivatives of the heavier elements at normal temperatures and pressure to oligomeric or polymeric aggregates. The significance of this last point is underlined by the brief but checkered history of arsenic trifluoride oxide. Thus a product with the composition $OAsF_3$ formed by thermal decomposition of the fluoride nitrate $AsF_3(NO_3)_2$ is described as a "white hygroscopic solid" involatile at ambient temperatures;[5] on the other hand, fluorination of an equimolar mixture of arsenic(III) chloride and arsenic(III) oxide is claimed elsewhere[6] to give a product also with this composition, which is a liquid with a boiling point of 26 °C.

The experience gained in several laboratories testifies to the feasibility of inducing oxygen atom transfer to a suitable molecular substrate by ultraviolet photolysis of ozone coexisting in a noble-gas matrix. Hence, for example, the molecules OClF[7] and HOX (X = Cl,[8] Br,[8] I[9]) have been generated from the substrates ClF and HX, respectively. Experiments carried out in this laboratory demonstrate that the matrix reaction

$$O_3 + D \xrightarrow{h\nu} DO + O_2$$

can also be enacted with either a group 5 trihalide[10,11] or iodine monochloride[12] as the donor partner D. We have established, for instance, that the hitherto unknown arsenic trichloride oxide, $OAsCl_3$, is formed by ultraviolet photolysis of a noble-gas matrix containing ozone and arsenic trichloride.[10,11] Seppelt and his co-workers[13] have exploited thermal rather than photolytic activation of the reaction between ozone and arsenic trichloride to synthesize arsenic trichloride oxide on a larger scale and so characterize it as a molecular solid stable at temperatures up to ca. −30 °C. They have also noted that ozone and arsenic trifluoride do not react in comparable circumstances.

In this paper we describe the formation of the molecules OPF_3 and $OAsF_3$ by ultraviolet photolysis of ozone supported in a noble-gas matrix doped with the appropriate trifluoride. We have witnessed the reaction and characterized each of the

---

(1) (a) Presented in part at the 6th European Symposium on Fluorine Chemistry, Dortmund, West Germany, March–April 1977. (b) Present address: Esso Research Centre, Abingdon, Oxfordshire OX13 6AE, England.

(2) Fox, W. B.; MacKenzie, J. S.; McCarthy, E. R.; Holmes, J. R.; Stahl, R. F.; Juurik, R. *Inorg. Chem.* **1968**, *7*, 2064. Plato, V.; Hartford, W. D.; Hedberg, K. *J. Chem. Phys.* **1970**, *53*, 3488.

(3) Toy, A. D. F. "The Chemistry of Phosphorus"; Pergamon Press: Oxford, 1975; p 430.

(4) Appelman, E. H. *Acc. Chem. Res.* **1973**, *6*, 113.

(5) Dehnicke, K.; Weidlein, J. *Z. Anorg. Allg. Chem.* **1966**, *342*, 225.

(6) Mitra, G. *J. Am. Chem. Soc.* **1958**, *80*, 5639.

(7) Andrews, L.; Chi, F. K.; Arkell, A. *J. Am. Chem. Soc.* **1974**, *96*, 1997.

(8) Schwager, I.; Arkell, A. *J. Am. Chem. Soc.* **1967**, *89*, 6006.

(9) Walker, N.; Tevault, D. E.; Smardzewski, R. R. *J. Chem. Phys.* **1978**, *69*, 564.

(10) Gaskill, G. P. D.Phil. Thesis, University of Oxford, 1978. Downs, A. J.; Gaskill, G. P.; Saville, S. B., unpublished results.

(11) Downs, A. J.; Gaskill, G. P. *Proc. Int. Conf. Raman Spectrosc. 5th* **1976**, 130. Benfield, F. W. S.; Downs, A. J.; Gaskill, G. P.; Staniforth, S. E. *J. Chem. Soc., Chem. Commun.* **1976**, 856.

(12) Drury, D. J. D.Phil. Thesis, University of Oxford, 1979. Downs, A. J.; Drury, D. J., unpublished results.

(13) Seppelt, K. *Angew. Chem., Int. Ed. Engl.* **1976**, *15*, 766. Seppelt, K.; Lentz, D.; Eysel, H.-H. *Z. Anorg. Allg. Chem.* **1978**, *439*, 5.

Table I. Wavenumbers and Intensities of the Infrared Absorptions due to Matrix-Isolated MF_3 Molecules (M = P, As)[a]

PF_3			AsF_3				
Ar matrix[b]	Kr matrix[b]	gas phase[c]	Ar matrix[b]	Kr matrix[b]	gas phase[c,d]	liquid[d]	assign and approx description of mode
885.5 884.0 } m[e]	882.3 m	892	730.6 m	730.4 m	740	715	ν_1 (a_1), sym ν(M-F)
850.1 848.7 s[e]	846.4 s	860	689.1 s	689.3 s	702	644	ν_3 (e), antisym ν(M-F)
487.3 484.7 } m[e]	486.5 m	487	338.7 m	338.2 m	336.5	342	ν_2 (a_1), sym $\delta(MF_3)$
348.6 w	349.2 w	344	267.3 w	263.1 w	262	280	ν_4 (e), antisym $\delta(MF_3)$

[a] Key: s, strong; m, medium; w, weak. [b] This work; error limits ±0.2 cm^{-1}. [c] Reference 14. [d] Reference 16. [e] Splitting attributed to occupation of more than one type of matrix site.

products by reference to the infrared spectrum of the matrix. By performing experiments with ^{18}O-enriched ozone, we have been able to verify the stoichiometry and geometry of the product and to explore its vibrational properties. We have also estimated the intensities of the absorptions principally associated with the M=O and M—F stretching fundamentals and sought to relate these to the bond angles in the OMF_3 molecule (M = P or As).

Infrared Spectra of the Molecules PF_3 and AsF_3 Isolated in Noble-Gas Matrices

When isolated in either an argon or a krypton matrix, typically at a ratio noble gas:PF_3 = (1000–2000):1, phosphorus trifluoride gave an infrared spectrum that included satellites on the low-energy side of each of the two intense bands attributable to the P–F stretching modes of monomeric PF_3. As the noble gas:PF_3 matrix ratio was reduced, so these additional features grew in intensity relative to the bands originating in the monomer; accordingly we associate them with aggregates of PF_3 molecules. All four fundamentals of the matrix-isolated PF_3 monomer have been located, with frequencies close to those of the gaseous molecule[14] and matching well the results of matrix-isolation experiments previously reported[15] (see Table I).

Similar experiments aimed at characterizing the infrared spectrum of the monomeric AsF_3 molecule revealed an even greater proclivity to aggregation effects. Thus, annealing a krypton matrix at 38 K was seen to result not only in a reduction in the intensity of the two most prominent absorptions near 730 and 690 cm^{-1} (attributed respectively to ν_1 (a_1) and ν_3 (e) of monomeric AsF_3) but also in the appearance and growth of a new feature at 667.6 cm^{-1}. The origin of this feature in an As—F stretching mode of an aggregate $(AsF_3)_n$ is substantiated by comparison with the spectrum characteristic of liquid arsenic(III) fluoride[16] (see Table I). The frequencies of all four fundamentals of the matrix-isolated AsF_3 molecule are close to those ascribed to the gaseous molecule.[14]

Although ultraviolet photolysis of molecular fluorides has served as a means of eliminating fluorine atoms to give lower valent fluorides,[17] neither of the matrix-isolated trifluorides PF_3 and AsF_3 appeared to undergo any change when irradiated with the unfiltered output of a high-pressure mercury arc. Such a result is consistent with the absence of any electronic transitions in the gaseous molecules at wavelengths exceeding 200 nm;[18] it also confirmed the suitability of the molecules as potential substrates for oxygen atom transfer, providing clear access to the ultraviolet and visible absorption bands of ozone[19] and presenting no obvious pathways to compete with the desired photochemical change, i.e.

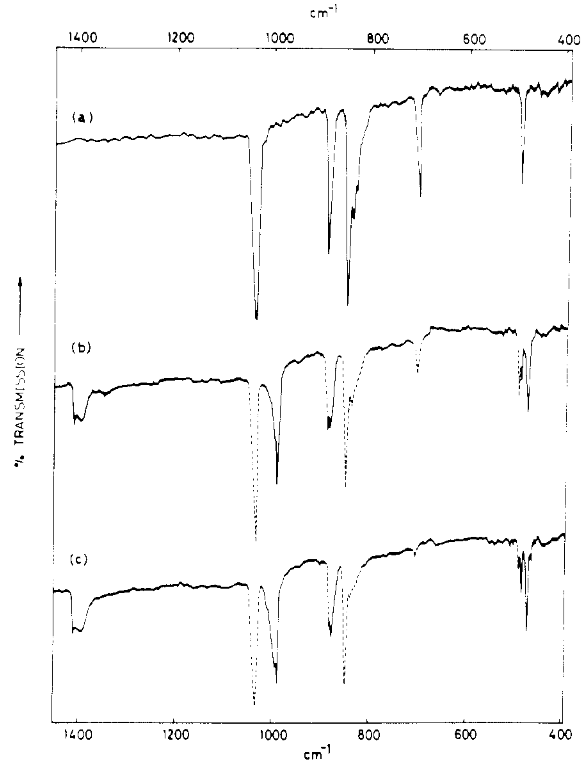

Figure 1. Infrared spectra of (a) the condensate formed by isolating phosphorus(III) fluoride and ozone in solid krypton at 20 K, (b) the same condensate after ultraviolet photolysis for 10 min at 20 K, and (c) the same condensate after ultraviolet photolysis for a further 30 min at 20 K: (---) features due to unchanged PF_3 and O_3; (—) features that develop on photolysis and that are attributed to OPF_3.

$$O_3 + MF_3 \xrightarrow[M = P, As]{h\nu} OMF_3 + O_2 \qquad (1)$$

Formation of the Trifluoride Oxide Molecules OMF_3 (M=P, As) by Ultraviolet Photolysis of Noble-Gas Matrices Including Ozone with the Trifluoride MF_3

(i) OPF_3. Throughout the series of photolysis experiments involving phosphorus(III) fluoride and ozone, argon or krypton was used as the matrix support. In either case the incorporation of ozone, typically with noble gas:O_3:PF_3 ratios of 2000:20:1, resulted in a broadening of the two absorptions due to the P–F stretching fundamentals of the trifluoride. Indeed, with a krypton matrix it was possible to detect the development in the presence of ozone of new, distinct bands on the low-

---

(14) Clark, R. J. H.; Rippon, D. M. *J. Mol. Spectrosc.* **1974**, *52*, 58.

(15) Perutz, R. N.; Turner, J. J. *J. Chem. Soc., Faraday Trans. 2* **1973**, *69*, 452.

(16) Brieux de Mandirola, O. *J. Mol. Struct.* **1969**, *3*, 465. Evans, J. A.; Long, D. A. *J. Chem. Soc. A* **1968**, 1688.

(17) See for example: Burdett, J. K.; Turner, J. J. "Cryochemistry"; Moskovits, M., Ozin, G. A., Eds.; Wiley: New York, NY, 1976; p 502. Andrews, L. *J. Chem. Phys.* **1972**, *57*, 51. Jacox, M. E.; Milligan, D. E.; Guillory, W. A.; Smith, J. J. *J. Mol. Spectrosc.* **1974**, *52*, 322. Smardzewski, R. R.; Fox, W. B. *J. Fluorine Chem.* **1976**, *7*, 353, 453, 456. Paine, R. T.; McDowell, R. S.; Asprey, L. B.; Jones, L. H. *J. Chem. Phys.* **1976**, *64*, 3081.

(18) McAdams, M. J.; Russell, B. R. *Chem. Phys. Lett.* **1973**, *18*, 402. Hawkins, M.; Reynolds, H. E., unpublished results.

(19) Inn, E. C. Y.; Tanaka, Y. *J. Opt. Soc. Am.* **1953**, *43*, 870.

Table II. Wavenumbers and Intensities[a] of the Infrared Absorptions due to the OPF_3 Molecule As Formed by the Photolysis of a Noble-Gas Matrix Doped with a Mixture of O_3 and PF_3

Ar matrix[b]		Kr matrix[b]	gas phase[c]	
$^{16}OPF_3$	$^{18}OPF_3$	$^{16}OPF_3$	$^{16}OPF_3$	assignt and approx description of mode
1410.3 w	1370.9 w	1407.6 w	1416.8 w	ν_1 (a_1), ν(P=O)
989.9 vs	989.1 vs	988.7 vs	991.0 vs	ν_4 (e), antisym ν(P–F)
873.9 m	866.2 m	873.8 m	872.7 m	ν_2 (a_1), sym ν(P–F)
482.1 m	477.0 m	481.0 m	482.0 m	ν_3 (a_1), sym $\delta(PF_3)$
471.3 m	463.2 m	469.4 m	472.4 m	ν_5 (e) } antisym $\delta(PF_3) + \rho(PF_3)$[f]
(329.0 vw)[d]	(327.0)[e]		335.5 vw	ν_6 (e) }

[a] Key: s, strong; m, medium; w, weak; v, very. [b] Frequency error limits ±0.2 cm^{-1}. [c] Reference 23: frequencies derived from the Raman spectrum of the vapor. [d] For OPF_3 isolated in an argon matrix at 20 K with Ar:OPF_3 ≈ 100:1; error limits ±1.0 cm^{-1}. [e] Value estimated on the basis of normal-coordinate calculations. [f] Motions strongly coupled.

frequency side of each of the P–F stretching fundamentals. The bands due to matrix-isolated ozone tallied with those reported elsewhere,[20] but there were signs of broadening or the development of multiplet patterns caused by the simultaneous presence in the matrix of phosphorus trifluoride. The significance of these observations in relation to the mechanism of the photolytic change subsequently seen to occur will be discussed in a second paper.[21]

Figure 1 illustrates the effects of broad-band ultraviolet photolysis on the infrared spectrum of a krypton matrix containing phosphorus(III) fluoride and ozone. The spectrum of such a matrix disclosed the appearance and growth with photolysis of five new absorptions near 1410, 990, 870, 480, and 470 cm^{-1} with the simultaneous decay of the absorptions due to the PF_3 and O_3 molecules. Comparison of the frequencies and relative intensities of the new features with the infrared spectrum characteristic of gaseous phosphorus trifluoride oxide[22,23] leads inescapably to the conclusion that the photochemical reaction (1) takes place in these conditions to afford the OPF_3 molecule. A summary of the spectroscopic results derived for this product is contained in Table II. The absence from the spectrum of the matrix of an absorption corresponding to the fundamental of OPF_3 lowest in frequency (ca. 330 cm^{-1}) is scarcely surprising in the light of gas-phase measurements, which indicate that it is very weak.[22] Using a sample of phosphorus trifluoride oxide prepared by conventional means[24] and a relatively concentrated argon matrix at 20 K (Ar:OPF_3 = 100:1) has led subsequently to the location of this weak band at 329 ± 1 cm^{-1}.

Experiments with ^{18}O-enriched ozone confirmed the identity of OPF_3 as one of the products of the matrix reaction, yielding frequencies consistent with the vibrational assignment given in Table II but at variance with the assignment previously favored.[22,23]

We have also made use of the infrared spectra to estimate the relative intensities of the three absorptions associated mainly with the P═O and P—F bond-stretching fundamentals (ν_1 (a_1), ν_2 (a_1), and ν_4 (e)) of the OPF_3 molecule. Complications in the spectra of the photolyzed matrices caused by the overlap of ν_2 (a_1) of OPF_3 (at 874 cm^{-1}) with ν_1 (a_1) of unchanged PF_3 (at 885 cm^{-1}) were avoided by reference to the spectra of matrices produced by the pulsed deposition of premixed samples of the noble gas and OPF_3. Even so it was necessary to allow for the doublet structure of the absorption associated with ν_1 (a_1) of the entrapped OPF_3 molecule and also for satellites arising not from the monomer but from aggregates of OPF_3.

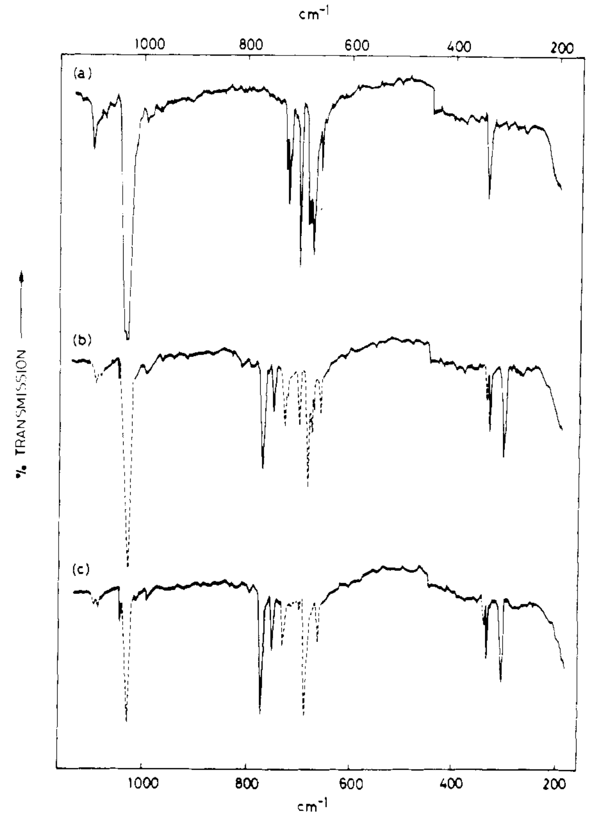

Figure 2. Infrared spectra of (a) the condensate formed by isolating arsenic(III) fluoride and ozone in solid krypton at 20 K, (b) the same condensate after ultraviolet photolysis for 10 min at 20 K, and (c) the same condensate after ultraviolet photolysis for a further 30 min at 20 K: (---) features due to unchanged AsF_3 and O_3; (—) features that develop on photolysis and that are attributed to $OAsF_3$.

(ii) $OAsF_3$. The introduction of ozone into an argon matrix containing arsenic(III) fluoride, typically with a ratio Ar:O_3:AsF_3 = 5000:50:1, resulted in a significant broadening of the infrared absorptions attributable to monomeric AsF_3, the effect being particularly pronounced on the low-frequency side of each of the two intense bands associated with the As–F stretching fundamentals. When the matrix was exposed to unfiltered ultraviolet radiation, the infrared spectrum underwent marked changes clearly expressive of a photochemical reaction between the trifluoride and ozone. Simultaneous with a reduction in the intensity of the infrared absorptions attributable to the AsF_3 and O_3 molecules were the appearance and growth of four new bands located at 774.3, 752.5, 333.4, and 306.8 cm^{-1}. Investigation of the growth and decay of band intensities established the common origin of the features which developed with photolysis.

Replacement of argon as the matrix support by krypton resulted in a considerable sharpening of the spectral features arising from the matrix-isolated species. Hence, whereas the

---

(20) Brewer, L.; Wang, J. L.-F. *J. Chem. Phys.* **1972**, *56*, 759. Andrews, L.; Spiker, R. C., Jr. *J. Phys. Chem.* **1972**, *76*, 3208. Spoliti, M.; Cesaro, S. N.; Mariti, B. *J. Chem. Phys.* **1973**, *59*, 985.

(21) Part 2: Downs, A. J.; Gaskill, G. P., to be submitted for publication.

(22) Selig, H.; Claassen, H. H. *J. Chem. Phys.* **1966**, *44*, 1404.

(23) Clark, R. J. H.; Rippon, D. M. *Mol. Phys.* **1974**, *28*, 305.

(24) Hayek, E.; Aignesberger, A.; Engelbrecht, A. *Monatsh. Chem.* **1955**, *86*, 735.

Table III. Wavenumbers[a] and Intensities[b] of the Infrared Absorptions due to the $OAsF_3$ Molecule as Formed by the Photolysis of a Noble-Gas Matrix Doped with a Mixture of O_3 and AsF_3

Ar matrix	Kr matrix		assignt and approx description of mode
$^{16}OAsF_3$	$^{16}OAsF_3$	$^{18}OAsF_3$	
1045.5 w[c]	1044.3 w	998.6 w	ν_1 (a_1), ν(As=O)
774.3 s	773.4 s	772.9 s	ν_4 (e), antisym ν(As–F)
752.5 m	751.5 m	747.3 m	ν_2 (a_1), sym ν(As–F)
333.4 m	332.9 m	331.9 m	ν_3 (a_1), sym $\delta(AsF_3)$
306.8 m	306.2 m	302.1 m	ν_5 (e), antisym $\delta(AsF_3) + \rho(AsF_3)$[d]

[a] Frequency error limits ±0.2 cm^{-1}. [b] Key: s, strong; m, medium; w, weak. [c] Estimated value; band obscured by the absorption due to ν_3 of unchanged ozone. [d] Motions strongly coupled.

introduction of ozone into an argon matrix containing arsenic(III) fluoride resulted in a broadening of the absorptions associated with the fluoride, the introduction of ozone into a krypton matrix gave rise to distinct absorptions additional to those characteristic of the isolated AsF_3 and O_3 molecules. The likely relevance of these extra features is elaborated later.[21] The changes in the infrared spectrum brought about by ultraviolet irradiation of such a matrix, illustrated in Figure 2, paralleled those displayed by an argon matrix in similar circumstances. Photolysis was seen to be attended in this case, however, by the development of an additional weak band at 1044.3 cm^{-1}, the intensity of which varied in unison with those of the four new bands near 770, 750, 330, and 305 cm^{-1}. Argon matrices gave no hint of a counterpart to this band presumably because it was masked by the relatively broad envelope of the intense absorption centered at 1035 cm^{-1} arising from ν_3 of the ozone molecules that survived photolysis.

A significant reduction in frequency of three out of the five new features was apparent when ^{18}O-enriched ozone was used in place of the isotopically natural reagent. Taken in conjunction (i) with the circumstances of the experiments, (ii) with the precedents established by the matrix reaction between ozone and phosphorus trifluoride and by the infrared spectrum of the gaseous molecule OVF_3,[22,23] and (iii) with the number, frequencies, and intensities of the new infrared absorptions, this evidence lends cogent support to the conclusion that the new molecule $OAsF_3$, presumably possessing C_{3v} symmetry, is formed in accordance with the photochemical reaction (1). The frequencies, intensities, and likely assignments of the absorptions attributable to this product are summarized in Table III.

Allowing the temperature of the matrix to rise resulted in a deterioration of its optical quality, but apart from some broadening of the bands, no significant changes in the infrared spectrum of the photolysis product could be discerned at temperatures up to 50 K, the point at which a krypton matrix starts to evaporate.

Vibrational Assignments of the Molecules OMF_3 (M = P, As)

(i) Stretching Modes. Usually well separated from the deformation modes by a frequency interval on the order of 200 cm^{-1}, the three bond-stretching fundamentals (2 a_1 + e) of a molecule of the type OMX_3 belonging to the C_{3v} point group have a characteristic frequency pattern that does not appear to vary with the nature of either the central atom M or the halogen atom X .[22,23,25,26] Highest in energy is ν_1 (a_1), a vibration approximating closely to the stretching motion of the multiply bonded M=O unit. Somewhat lower in energy come the two M—X stretching modes, ν_2 (a_1) and ν_4 (e), in the order $\nu_4 > \nu_2$. The four molecules OPF_3, $OAsF_3$, $OAsCl_3$, and $OPCl_3$ generated by oxygen atom transfer in low-temperature matrices[10,11] comply with this pattern, and the synthesis in these conditions of the ^{18}O-enriched compounds verifies that the infrared absorption highest in frequency originates predominantly in the M=O stretching fundamental. The finding that the lower frequency of the two absorptions attributable to the M—F stretching fundamentals of OPF_3 and $OAsF_3$ suffers a small but significant change in energy with ^{18}O enrichment likewise vindicates its assignment to the a_1 mode ν_2. That there is coupling between ν_1 and ν_2 is made plain on ^{18}O enrichment not only by the reduction in frequency of the band associated with ν_2 (isotopic shift 7.7 cm^{-1} for OPF_3 and 4.2 cm^{-1} for $OAsF_3$) but also by the fact that the corresponding shift in ν_1 (39.4 cm^{-1} for OPF_3 and 45.7 cm^{-1} for $OAsF_3$) falls short of the value predicted in the absence of coupling between the M=O and MF_3 oscillators (52.6 and 49.0 cm^{-1}, respectively).

(ii) Deformation Modes. For an OMX_3 molecule having halogen atoms that are moderately massive compared with the central atom M (i.e., X = Cl, Br), the infrared spectrum of the vapor reveals band contours typical of the perpendicular-type vibrations of an oblate symmetric top[27] for two of the three absorptions that occur in the region associated with the deformation modes of the molecule (350–100 cm^{-1}). On this basis, the absorptions are presumed to be due to the e fundamentals ν_5 and ν_6 which occur respectively at the upper and lower limits of the deformation region. The third feature intermediate in frequency exhibits the characteristics of a parallel-type vibration[27] and is therefore ascribed to ν_3 (a_1). This assignment finds support in analogous studies of the Raman spectra of such molecules; of the three lines attributable to the deformation modes, that intermediate in frequency is found to be polarized.[23] As the mass of the halogen decreases in relation to that of the central atom M, there is a decrease in the frequency separating the symmetric and antisymmetric MX_3 deformation modes. The near-degeneracy of these two fundamentals in OPF_3 makes it difficult to identify the correct assignment of the two bands to which they correspond in the vibrational spectrum of the vapor. There is little help to be gained, moreover, from the Raman spectrum in that all three of the lines arising from the deformation modes now appear to be depolarized.[23] This behavior, along with the weakness in infrared absorption of one of the deformation modes, is a sign of the T_d symmetry latent in a molecule of the type OMF_3 and reflecting the similarity in mass of the oxygen and fluorine ligands;[28] thus it underlines the parentage of the deformation modes of the C_{3v} molecule, viz., ν_2 (e, T_d) $\rightarrow$ ν_6 (e, C_{3v}) and ν_4 (t_2, T_d) $\rightarrow$ ν_3 (a_1, C_{3v}) + ν_5 (e, C_{3v}). The assignment favored by Selig and Claassen[22] and Clark and Rippon[23] relies upon the P–R separations exhibited by the relevant bands in the infrared and Raman spectra of the vapor.

With the additional information about the ^{18}O-substituted molecules afforded by our experiments, product-rule and normal-coordinate calculations offer the prospect of a more or less definitive vibrational assignment. On the evidence of these calculations, we are led to conclude that the assignment of ν_3 (a_1) and ν_5 (e) hitherto favored[22,23] for the OPF_3 molecule should be reversed and that ν_3 (a_1) of both OPF_3 and $OAsF_3$ should be allocated a frequency higher than that of ν_5 (e). On the other hand, we have been unable in the experiments performed to date to locate ν_6, the lower in frequency of the two degenerate deformation modes, for $OAsF_3$ as formed by

---

(25) Nakamoto, K. "Infrared and Raman Spectra of Inorganic and Coordination Compounds", 3rd ed.; Wiley-Interscience: New York, 1978; p 144.

(26) Müller, A.; Kebabcioglu, R.; Krebs, B.; Glemser, O. *Z. Phys. Chem. (Leipzig)* **1969**, *240*, 92.

(27) Seth-Paul, W. A. *J. Mol. Struct.* **1969**, *3*, 403.

(28) Edgell, W. F. *Spectrochim. Acta, Part A* **1975**, *31A*, 1623.

Table IV. Product-Rule Calculations for Different Assignments of the a_1 Fundamentals of the Molecules OMF_3 (M = P, As)

molecule	assignt	isotopic species	obsd freq, cm^{-1} ν_1	ν_2	ν_3	obsd product-rule ratio, P_{obsd}[c]	theor product-rule ratio, P_{theor}[d]	$(P_{obsd} - P_{theor})/P_{theor}$, %
OPF_3[a]	A	$^{16}OPF_3$	1410.3	873.9	482.1	0.953 31	0.951 83	+0.15
		$^{18}OPF_3$	1370.9	866.2	477.0			
	B	$^{16}OPF_3$	1410.3	873.9	471.3	0.946 94	0.951 83	−0.51
		$^{18}OPF_3$	1370.9	866.2	463.2			
$OAsF_3$[b]	A	$^{16}OAsF_3$	1044.5	751.5	332.9	0.947 86	0.949 16	−0.14
		$^{18}OAsF_3$	998.6	747.3	331.9			
	B	$^{16}OAsF_3$	1044.5	751.5	306.2	0.938 07	0.949 16	−1.18
		$^{18}OAsF_3$	998.6	747.3	302.1			

[a] Ar matrix. [b] Kr matrix. [c] $P_{obsd} = \nu_1\nu_2\nu_3(^{18}OMF_3)/\nu_1\nu_2\nu_3(^{16}OMF_3)$. Experimental error limits ±0.23%. [d] As derived from the masses of the constituent atoms (eq 2).

Table V. Observed and Calculated Frequencies (in cm^{-1}) of the Molecules OPF_3 and $OAsF_3$ Isolated in Noble-Gas Matrices

		OPF_3				$OAsF_3$			
		$^{16}OPF_3$		$^{18}OPF_3$		$^{16}OAsF_3$		$^{18}OAsF_3$	
symm class	fundamental	obsd[a]	calcd[b,c]	obsd[a]	calcd[b,c]	obsd[d]	calcd[e,f]	obsd[d]	calcd[e,f]
a_1	ν_1	1410.3	1410.5	1370.9	1370.7	1044.3	1044.5	998.6	998.4
	ν_2	873.9	874.0	866.2	866.1	751.5	751.7	747.3	747.2
	ν_3	482.1	482.3	477.0	476.8	332.9	332.6	331.9	332.2
e	ν_4	989.9	990.2	989.1	988.8	773.4	773.2	772.9	773.1
	ν_5	471.3	471.5	463.2	463.0	306.2	306.1	302.1	302.2
	ν_6	329.0[g]	329.3	(327.0)[h]	326.7	(286.3)[h]	286.2	(280.9)[h]	281.0

[a] Ar matrix at 12 K; frequency error limits ±0.2 cm^{-1}. [b] Calculated on the basis of the following dimensions: r(P=O) = 144 pm; r(P–F) = 152 pm; ∠FPF = 101.3°.[31] [c] Rms error between observed and calculated frequencies 0.21 cm^{-1}. [d] Kr matrix at 12 K; frequency error limits ±0.2 cm^{-1}. [e] Calculated on the basis of the following estimated dimensions: r(As=O) = 157 pm; r(As–F) = 168 pm; ∠FAsF = 98°. [f] Rms error between observed and calculated frequencies 0.21 cm^{-1}. [g] Concentrated Ar matrix at 20 K; frequency error limits ±1.0 cm^{-1}. [h] Too weak in infrared absorption to be detected.

oxygen atom transfer in a low-temperature matrix. This failure may be attributed either to the low intensity of the corresponding infrared absorption (cf. OPF_3) or to its location outside the range of the spectrometer used (cf. $OAsCl_3$[10,11,13]).

(iii) Product-Rule Calculations. The frequencies of the nondegenerate fundamentals for two different isotopic versions of a ZMX_3 molecule each possessing C_{3v} symmetry are related to the masses of the constituent atoms by (2), where $\sum m =$

$$\frac{\nu_1{}^i\nu_2{}^i\nu_3{}^i}{\nu_1\nu_2\nu_3} = \frac{m_X}{m_X{}^i}\left(\frac{m_Z m_M \sum m^i}{m_Z{}^i m_M{}^i \sum m}\right)^{1/2} \qquad (2)$$

$m_Z + m_M + 3m_X$ and all the quantities referring to the second isotopomer are marked by the superscript "i". The theoretical product-rule ratio derived from the masses of the constituent atoms has thus been calculated for the species $^{16}OMF_3$ and $^{18}OMF_3$ (where M = P or As) and compared with the observed ratio based on each of two different assignments for the mode ν_3. Any comparison between the theoretical and observed ratios must acknowledge, however, that eq 2 holds rigorously only for the frequencies appropriate to a harmonic oscillator; use of anharmonic rather than harmonic frequencies is likely to give an observed frequency ratio $\nu_1\nu_2\nu_3(^{18}OMF_3)/\nu_1\nu_2\nu_3(^{16}OMF_3)$ slightly *in excess of* the theoretical ratio.[29] Accordingly, the difference between the observed and theoretical ratios shown in Table IV should have a *positive* sign. Consideration of the magnitude and sign of this difference clearly favors for OPF_3 the assignment in which the higher frequency deformation mode corresponds to ν_3 (a_1). Although the analogous assignment for $OAsF_3$ produces an observed frequency ratio slightly *smaller* than the theoretical ratio, the discrepancy is well within the limits of experimental error (±0.23%). By contrast, the observed ratio implied by the alternative assignment (B) falls short of the theoretical ratio by a margin that strays beyond the limits of experimental error. In fact, the magnitude of the anharmonicity correction may be gauged by assuming an anharmonicity factor, x_{ik}, of 2% for each of the a_1 frequencies of $^{16}OAsF_3$ and then using the Darling–Dennison relationship[30] to calculate the corresponding factors, $x_{ik}{}^{(i)}$, for $^{18}OAsF_3$. Although this probably overestimates the magnitude of the anharmonicity terms, it emerges that the errors in the product-rule calculations incurred through the use of anharmonic rather than harmonic frequencies amount to no more than 0.08%, well within the limits of experimental error.

Our conclusions are summarized by the line diagram of Figure 3, which compares schematically the frequencies, relative intensities, and assignments of the infrared absorptions due to the vibrational fundamentals of the six trihalide oxide molecules OPF_3, OVF_3, $OAsF_3$, $OPCl_3$, $OVCl_3$, and $OAsCl_3$.

Normal-Coordinate Analysis of the Molecules OMF_3 (M = P, As)

Using the vibrational assignments to which we are led by the arguments given in the preceding section, we have carried out a normal-coordinate analysis on the molecules OPF_3 and $OAsF_3$. This we have based on the internal coordinates specified in Figure 4 and the structural parameters summarized at the foot of Table V; the dimensions of the OPF_3 molecule have been established by electron diffraction measurements,[31] whereas those of the $OAsF_3$ molecule have been derived either by reference to the internuclear distances in related species, e.g., AsF_3,[32,33] AsF_5,[32] and $AsO_4{}^{3-}$,[34] or by calculations involving the approximate stretching force constants or the relative intensities of the infrared absorptions

---

(29) Herzberg, G. "Infrared and Raman Spectra of Polyatomic Molecules"; Van Nostrand: Princeton, NJ, 1945; p 232.

(30) Darling, B. T.; Dennison, D. M. *Phys. Rev.* **1940**, *57*, 128.

(31) Moritani, T.; Kuchitsu, K.; Morino, Y. *Inorg. Chem.* **1971**, *10*, 344.

(32) Clippard, F. B., Jr.; Bartell, L. S. *Inorg. Chem.* **1970**, *9*, 805.

(33) Konaka, S. *Bull. Chem. Soc. Jpn.* **1970**, *43*, 3107.

(34) Vansant, F. K.; van der Veken, B. J. *J. Mol. Struct.* **1973**, *15*, 439. Van der Veken, B. J.; Vansant, F. K.; Herman, M. A. *Ibid.* **1977**, *36*, 225.

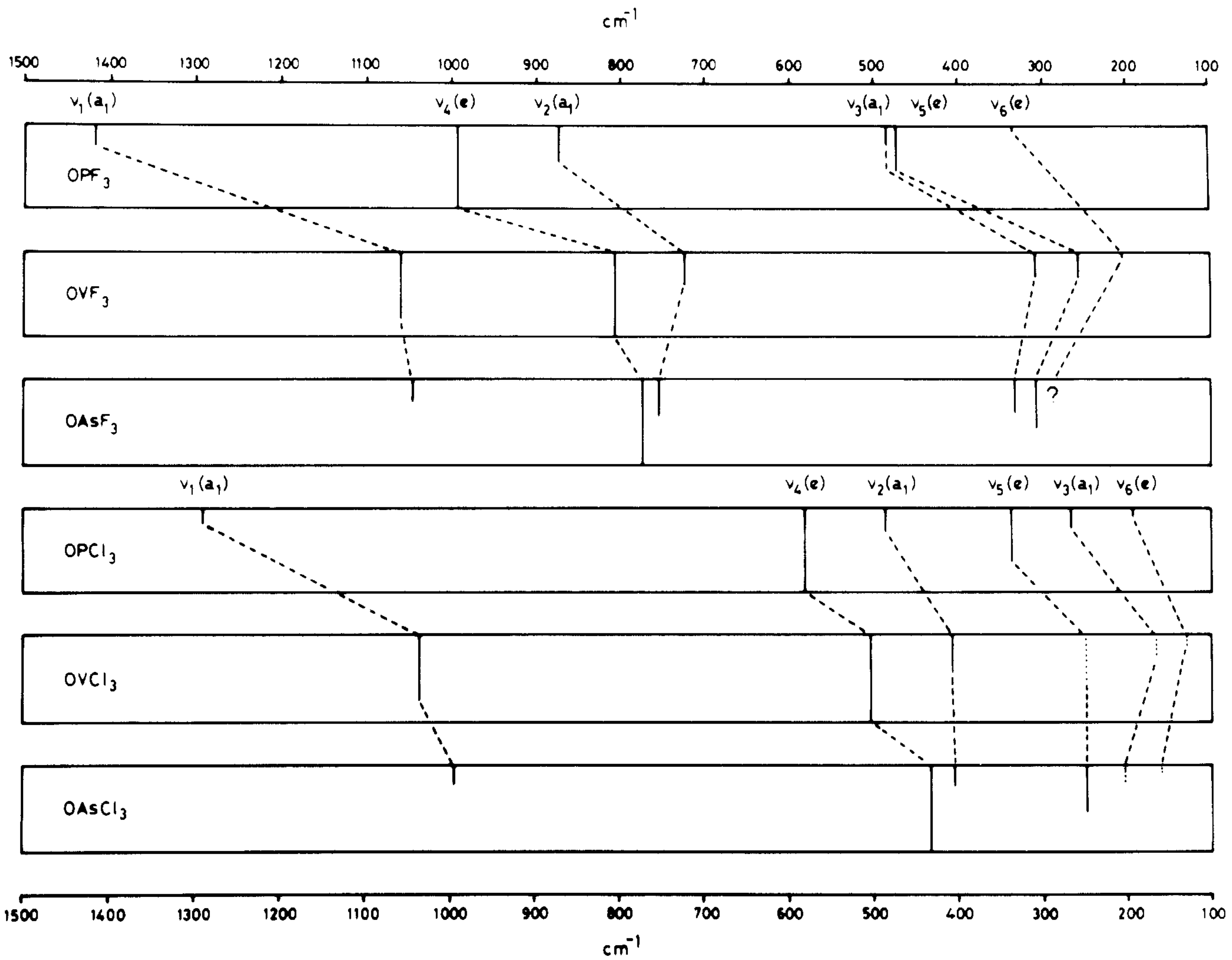

Figure 3. Line diagram depicting the principal features in the region 100–1500 cm^{-1} of the infrared spectra displayed by gaseous or matrix-isolated molecules of the type OMX_3 (M = P, V, As; X = F, Cl).

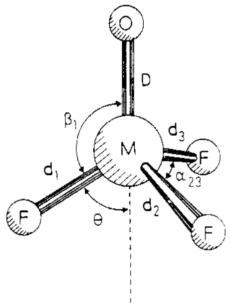

Figure 4. Internal coordinates used in the force field analysis of molecules of the type OMF_3 (M = P, As).

Table VI. Summary of the Force Constants Deduced for the Molecules OPF_3 and $OAsF_3$ Isolated in Noble-Gas Matrices

F-matrix element or valence force const[a]	molecule	
	OPF_3	$OAsF_3$
F_{11}	1102.020	857.018
F_{12}	16	0
F_{13}	25	−80
F_{22}	761.302	555.535
F_{23}	68	0
F_{33}	142.909	98.362
F_{44}	574.777	510.364
F_{45}	−36	0
F_{46}	−80	0
F_{55}	142.804	112.035
F_{56}	−23	0
F_{66}	122.516	75.089
f_D	1102	857
f_d	637	525
f_{dd}	62	15
f_{dD}	9	0
$f_\alpha - f_{\alpha\alpha}$	53	42
$f_\beta - f_{\beta\beta}$	65	27

[a] Units: $F_{11}, F_{12}, F_{22}, F_{44}$, N m^{-1}; $F_{13}, F_{23}, F_{45}, F_{46}$, N rad^{-1}; $F_{33}, F_{55}, F_{56}, F_{66}$, N m rad^{-2}; $f_D, f_d, f_{dd}, f_{dD}, f_\alpha, f_{\alpha\alpha}, f_\beta, f_{\beta\beta}$, N m^{-1}. The subscripts of the valence force constants refer to the internal coordinates defined in Figure 4.

originating in the bond-stretching fundamentals of the molecule (quod vide). A simple valence force field with zero off-diagonal force constant values was first employed to accommodate the observed fundamental frequencies of the $^{16}OMF_3$ molecule (M = P, As). The frequency shifts attending ^{18}O substitution were then used to constrain the solution of the vibrational problem for OPF_3 on the basis of a general valence force field. A similar approach was adopted for the a_1 fundamentals of $OAsF_3$, but in the absence of any information about ν_6 (e), the analysis of the e block made use of nothing more elaborate than the simple valence force field. The optimum solutions give the results listed in Table V with a standard deviation between the observed and calculated frequencies amounting in both cases to 0.21 cm^{-1}; the corresponding force constants are summarized in Table VI. The analysis implies a reasonable measure of "energy factoring" for the individual a_1 modes; thus, according to the potential

Table VII. Principal Stretching Force Constants of $OAsF_3$ and Related Species

molecular species MO_mX_n	principal str force const, N m^{-1} M–O	principal str force const, N m^{-1} M–X	ref	molecular species MO_mX_n	principal str force const, N m^{-1} M–O	principal str force const, N m^{-1} M–X	ref
$OAsF_3$	857	525	this work	$OAsCl_3$	747	259	*f*
AsF_3		475	*a*	$AsCl_3$		231	*g*
AsF_5		446 (ax) 553 (eq)	*b*	OPF_3	1102	637	this work
AsF_6^-		372	*c*	PF_3		540	*h*
AsO_4^{3-}	493		*d*	OVF_3	780	498	*i*
$HOAsO_3^{2-}$	560 417		*d*	$OVCl_3$	760	275	*i*
$(HO)_2AsO_2^-$	605 472		*d*	VO_4^{3-}	459		*j*
$(HO)_3AsO$	639 520		*d*	SeO_4^{2-}	585		*j*
$CH_3AsO_3^{2-}$	506		*d*	SeO_2F_2	829	458	*k*
$(CH_3)_2AsO_2^-$	531		*d*	$OSeF_4$	820	410 (ax) 470 (eq)	*l*
$(CH_3)_3AsO$	576		*d*	BrO_4^-	605		*m*
As_4O_6	297		*e*	BrO_3F	692	322	*n*

[a] Reference 33. [b] Hoskins, L. C.; Lord, R. C. *J. Chem. Phys.* **1967**, *46*, 2402. Levin, I. W. *J. Mol. Spectrosc.* **1970**, *33*, 61. [c] Begun, G. M.; Rutenberg, A. C. *Inorg. Chem.* 1967, *6*, 2212. [d] Reference 34. [e] Müller, A.; Cyvin, B. N.; Cyvin, S. J.; Pohl, S.; Krebs, B. *Spectrochim. Acta, Part A* **1976**, *32A*, 67. [f] Reference 13. [g] Cazzoli, G.; Forti, P.; Lunelli, B. *J. Mol. Spectrosc.* **1978**, *69*, 71. [h] Reference 36. [i] Müller, A.; Krebs, B.; Fadini, A.; Glemser, O.; Cyvin, S. J.; Brunvoll, J.; Cyvin, B. N.; Elvebredd, I.; Hagen, G.; Vizi, B. *Z. Naturforsch., A* **1968**, *23*, 1656. [j] Krebs, B.; Müller, A.; Fadini, A. *J. Mol. Spectrosc.* **1967**, *24*, 198. [k] Ramaswamy, K.; Jayaraman, S. *J. Mol. Struct.* **1970**, *5*, 325. [l] Willert-Porada, M.; Willner, H.; Seppelt, K. *Spectrochim. Acta, Part A* **1981**, *37A*, 911. [m] Brown, L. C.; Begun, G. M.; Boyd, G. E. *J. Am. Chem. Soc.* **1969**, *91*, 2250. [n] Appelman, E. H.; Beagley, B.; Cruickshank, D. W. J.; Foord, A.; Rustad, S.; Ulbrecht, V. *J. Mol. Struct.* **1976**, *35*, 139.

energy distribution each of the modes ν_1, ν_2, and ν_3 of the molecules OPF_3 and $OAsF_3$ owes a contribution of at least 82% to the relevant symmetry coordinate. On the other hand, the similarity in the masses of oxygen and fluorine leads to pronounced coupling between the coordinates that define antisymmetric deformation of the MF_3 fragment and rocking of the OMF_3 skeleton; the extent of this is such that neither of the e deformation modes ν_5 and ν_6 can be described realistically in terms of a single symmetry coordinate.

The force constants listed in Tables VI and VII reveal nothing unusual or unforeseen in the force field of the $OAsF_3$ molecule suggestive of intrinsic weakness on the part of the As=O or As—F bonds. The closest analogy is provided by the gaseous molecule OVF_3, which is thermally stable at temperatures in excess of 100 °C[35] and which includes a central atom with a mass close to that of arsenic; here the principal stretching force constants are actually somewhat inferior to those we have deduced for the matrix-isolated $OAsF_3$ molecule, in keeping with the enhanced polarity of the bonds in which vanadium is engaged. That isolation in a noble-gas matrix of a molecule of this type has but a minimal effect on its vibrational properties is attested by the case of OPF_3, the principal absorptions of which vary in frequency by less than 0.5% with the transition from the gaseous to the matrix-isolated condition.

The replacement of phosphorus by arsenic as the central atom M in the trifluoride oxide molecule OMF_3 is attended not only by the expected decrease in the principal stretching force constants but also by a dramatic decrease in the interaction constant f_{dd} linking pairs of M–F bonds. This is the factor principally responsible for the narrowing of the frequency gap between the antisymmetric and symmetric M–F stretching fundamentals, ν_4 (e) and ν_2 (a_1), respectively, from 116 cm^{-1} in OPF_3 to 22 cm^{-1} in $OAsF_3$.

As in the transition from PF_3[36] to OPF_3, the attachment of oxygen to the AsF_3 molecule[33] to form $OAsF_3$ inflates the principal M–F stretching force constant (from 475 to 525 N m^{-1}), while having little effect on the MF_3 deformation force constant. For both OPF_3 and $OPCl_3$, this variation in the P–X stretching force constant is mirrored by a modest shortening of the P–X bond (e.g., from 157.0 pm in PF_3[37] to 152.4 pm in OPF_3[31]). We assume that a similar effect operates in $OAsF_3$ and are led, by the empirical expressions relating force constant to bond length developed by Badger,[38] Herschbach and Laurie,[39] or van der Veken et al.,[34] to the following estimates of bond length: r(As=O) = 157 pm and r(As—F) = 168 pm. The changes induced in the MX_3 fragment when M is additionally coordinated by an oxygen atom may be explained in terms of the effective lowering in energy of the valence s and p orbitals of M brought about when it acts as a σ donor with respect to the electronegative oxygen atom; this has the effect of reducing the energy difference between the orbitals based on M and those based on the halogen atoms X, implying enhanced bonding interactions between the different sets of orbitals. Alternatively the outcome may be viewed in terms of interaction between the two bonding orbitals common to the a_1 symmetry class in the valence shell of the OMX_3 molecule.

Determination of the Bond Angles in the Matrix-Isolated Molecules OMF_3 (M = P, As)

For neither of the matrix-isolated molecules OMF_3 (M = P, As), which we have prepared and characterized, do we have sufficient information about the frequencies of the fundamentals belonging to the e block to make an estimate of the interbond angles on the basis of a product-rule calculation. We have therefore resorted to measurements of infrared band intensities as a possible means of defining the geometry of the OMF_3 molecule.[40,41] Assuming that the M—F and M=O internal coordinates associated with bond-stretching fundamentals do not couple significantly with each other or with the other internal coordinates of the molecule leads to the

---

(35) "Gmelins Handbuch der Anorganischen Chemie"; Verlag Chemie: Weinheim/Bergstr., 1967; Part B (1), System No. 48, p 192.

(36) Hirota, E.; Morino, Y. *J. Mol. Spectrosc.* **1970**, *33*, 460.

(37) Morino, Y.; Kuchitsu, K.; Moritani, T. *Inorg. Chem.* **1969**, *8*, 867.

(38) Badger, R. M. *J. Chem. Phys.* **1934**, *2*, 128; **1935**, *3*, 710.

(39) Herschbach, D. R.; Laurie, V. W. *J. Chem. Phys.* **1961**, *35*, 458.

(40) Burdett, J. K.; Poliakoff, M.; Turner, J. J.; Dubost, H. *Adv. Infrared Raman Spectrosc.* **1976**, *2*, 1.

(41) Smit, W. M. A. *J. Mol. Struct.* **1973**, *19*, 789.

Table VIII. Estimation of Bond Angles[a] on the Basis of the Intensities in Infrared Absorption of the Stretching Fundamentals of MF_3 and OMF_3 Molecules

		intens ratios[b]		best estimates of angles		
molecule	matrix	$R_1^2 = I(M{=}O)/I(M{-}F)$	$R_2^2 = I(e)/I(a_1)$	θ,[c] deg	α,[c] deg	bond angle in the gaseous molecule α, deg
NF_3	Ar[d]		10.4 (2.6)	68 (3)[e]	107 (3)[e]	102.37 (0.03)[f]
PF_3	Ar, Kr		2.4 (0.6)	57 (4)[e]	93 (5)[e]	97.8 (0.2)[g]
AsF_3	Ar, Kr		3.6 (0.9)	61 (4)[e]	99 (5)[e]	96.2 (0.2)[h]
SbF_3	Kr[d]		3.2 (0.8)	60 (4)[e]	97 (5)[e]	
OPF_3	Ar	4.8 (1.2)	7.4 (1.9)	59 (5)[i]	96 (7)[i]	101.3 (0.2)[j]
$OAsF_3$	Kr	1.3 (0.6)	3.4 (0.9)	61 (4)[e,i]	98 (5)[e,i]	

[a] Values in parentheses are the estimated standard deviations. [b] See text. [c] Angles as defined in Figure 4. [d] Reference 10. [e] Based on eq 4 (see text). [f] Otake, M.; Matsumura, C.; Morino, Y. *J. Mol. Spectrosc.* 1968, *28*, 316. [g] Reference 37. [h] Reference 32. [i] Based on eq 5, out-of-phase solution (see text). [j] Reference 31.

following simple expression relating the semivertical angle θ (see Figure 4) to the intensities in infrared absorption I of the a_1 and e M–F stretching fundamentals:

$$\frac{I(e)}{I(a_1)} = \tan^2 \theta \qquad (3)$$

Allowance for the motion of the central atom yields a modified form of this equation involving the masses m of the atoms M and F,[42] viz.

$$\frac{I(e)}{I(a_1)} = (\tan^2 \theta)\frac{m_M + {}^3/_2 m_F \sin^2 \theta}{m_M + 3m_F \cos^2 \theta} \qquad (4)$$

Mixing between the a_1 stretching modes $\nu(M{=}O)$ and $\nu(M{-}F)$ may be taken into account by setting $R_1 = [I(M{=}O)/I(M{-}F)]^{1/2}$ for the a_1 modes and $R_2 = [I(e)/I(a_1)]^{1/2}$ for the M–F stretching modes to deduce that

$$\theta = \tan^{-1}\left[\frac{R_2(L_{11}L_{22} - L_{12}L_{21})}{L_{33}(L_{12}R_1 - L_{11})}\right] \qquad (5)$$

Calculations based on eq 3–5 and incorporating the measured intensities of the relevant bands exhibited by the matrix-isolated molecules NF_3, PF_3, AsF_3, SbF_3, OPF_3, and $OAsF_3$ yield the estimates of the semivertical and F–M–F bond angles listed in Table VIII. Equations 3 and 4 lead to bond angles for NF_3 and OPF_3 which are appreciably different from the observed values. This can be attributed, at least in part, to mixing of the M—F stretching with other vibrations (deformation modes in the case of NF_3 and the P=O stretching mode in the case of OPF_3). Application of eq 5 to the molecules OPF_3 and $OAsF_3$ requires a knowledge of the phasing of the intensities associated with the a_1 stretching modes $\nu(M{=}O)$ and $\nu(M{-}F)$.[40] Reference to the intensities of the bands due to ν_1, ν_2, and ν_4 of the molecules $^{18}OMF_3$ (M = P, As) does not reveal any clear-cut distinction between the in-phase and out-of-phase solutions although the results tend to favor the out-of-phase solution.

About the admissibility of any form of frequency-factoring doubts are bound to persist; indeed it is possible that the agreement between the calculated and observed bond angles of certain molecules[40,41] derives more from a fortuitous cancellation of terms than from a proper approximation to the idealized model on which the calculations are founded. There are in addition other features of the model which admit uncertainty.[40,41] Among these are the assumptions (i) that the fundamental modes in question exhibit both electrical and mechanical harmonicity, (ii) that the rotational motion of the molecule does not contribute to the intensity of absorption (implying the absence of a permanent dipole moment), and (iii) that the bond dipole moment vector coincides with the axis of the relevant bond.

The results at present available to us are insufficient to offer any obvious alternative to this approach for the evaluation of the interbond angles in matrix-isolated fluorides of the types MF_3 and OMF_3. The consensus of our evidence based on the relative intensities in infrared absorption of the bond-stretching fundamentals is that the F–As–F bond angle in the $OAsF_3$ molecule is 98 ± 5°.

Experimental Section

The principal features of the experiments corresponded to what is now familiar practice.[43] In outline, however, deposition of the matrices from the vapor phase took place on a CsI window cooled to 8–30 K by means of a Displex refrigerator (Air Products, Model CS 202) incorporated in a conventional high-vacuum system operating at a pressure less than 10^{-7} torr. Temperatures were measured with a chromel vs. iron-doped gold thermocouple or with a hydrogen vapor bulb.

Two methods were used to prepare the ozone. The first involved passing a stream of dried oxygen (commercial grade, 99.5% purity) through a silent electrical discharge and then adsorbing the ozone, typically present in a few mole percent, in a trap containing silica gel (30–120 mesh), which had been previously dried under pumping at 110 °C for several hours. Depending upon the amount of ozone required within the matrix, the temperature and time of adsorption could be varied. In a typical experiment, however, adsorption took place over a period of 15 min with the silica gel held at −15 °C. Desorption under reduced pressure was carried out at −78 °C. Whereas this method unquestionably yielded a high proportion of ozone to oxygen within the matrix, its scale was inappropriate for the preparation of ^{18}O-enriched ozone. As an alternative, an inert gas containing 2–5 mol % oxygen was passed at a pressure of ca. 1 torr through a microwave discharge produced by a Microtron Model 200 generator (Electro-Medical Supplies Ltd.) with a power dissipation in the gas typically in the order of 60 W. The presence of such impurities as carbon dioxide, water, and particularly nitrogen was apt to be troublesome with this approach, but thorough "flaming out" of the quartz discharge tube and operation of the discharge for a short time prior to cooling the CsI window served to condition the apparatus and so minimize the level of contamination. For a given experiment, the two methods of generating ozone yielded identical spectroscopic results. ^{18}O-enriched oxygen (Prochem, 99 atom % ^{18}O) was used without further purification.

Trap-to-trap distillation in vacuo of commercial phosphorus trifluoride (Strem Chemicals) gave a product judged to be pure on the basis of its vapor pressure and the infrared spectrum of its vapor. The purified trifluoride was invariably mixed with the matrix gas prior to condensation. The reaction of fluorosulfonic acid with arsenic(III) oxide[44] was used to prepare arsenic trifluoride. The infrared spectrum of the vapor contained in a Pyrex-bodied cell revealed traces of silicon tetrafluoride as the only detectable impurity after trap-to-trap distillation in vacuo of the crude trifluoride. Deposition of the arsenic

---

(42) Beattie, I. R.; Ogden, J. S.; Price, D. D. *J. Chem. Soc., Dalton Trans.* **1982**, 505.

(43) See for example: Hallam, H. E., Ed. "Vibrational Spectroscopy of Trapped Species"; Wiley: London, 1973.

(44) Engelbrecht, A.; Aignesberger, A.; Hayek, E. *Monatsh. Chem.* **1955**, *86*, 470.

trifluoride from glass apparatus was always accompanied by small amounts of silicon tetrafluoride, although the proportion of impurity seemed to decrease with time, presumably with progressive conditioning of the apparatus. No attempt was made to mix the trifluoride with the matrix gas prior to condensation; instead the trifluoride was vaporized from an ampule cooled to −72 °C and cocondensed with the matrix gas on the CsI window.

Phosphorus trifluoride oxide was prepared by the reaction between fluorosulfonic acid and phosphorus pentoxide[24] and purified by trap-to-trap distillation in vacuo. The infrared spectrum of the vapor revealed some contamination of the sample by sulfur dioxide and silicon tetrafluoride, but these did not appear to interfere with the matrix isolation of the OPF$_3$ molecule.

Matrices were formed normally by continuous (rather than pulsed) deposition; the deposition rate was in the order of 3 mmol of matrix gas/h, and deposition took place over periods varying from 30 min to more than 3 h. The photolysis source was a Hanovia Uvitron 125-W high-pressure mercury arc used in conjunction with a 4-cm quartz cell containing water to act as a heat filter.

Infrared spectra were recorded by using a Perkin-Elmer Model 225 spectrophotometer. Calibration was accomplished by superimposing on the measured spectrum sharp vibration-rotation or rotation lines due to ammonia, atmospheric water vapor, or carbon dioxide;[45] hence the frequencies of the bands due to the sample were calibrated by interpolation. Such measurements were reproducible within 0.2 cm^{-1} for sharp lines; the resolution was invariably better than 0.5 cm^{-1}. The relative intensities of infrared absorptions were measured either by taking the product of peak height and width at half-height or by tracing the peaks, cutting out, and weighing.

Normal-coordinate-analysis calculations were performed with the aid of an ICL 2980 digital computer by using programs kindly supplied by Professor H. Bürger and Dr. K. Burczyk of the Gesamthochschule Wuppertal.

Acknowledgment. G.P.G. acknowledges with thanks the award of research studentships by the Science Research Council and Linacre College, Oxford.

Registry No. OPF$_3$, 13478-20-1; OAsF$_3$, 15120-14-6; PF$_3$, 7783-55-3; AsF$_3$, 7784-35-2; O$_3$, 10028-15-6.

---

(45) IUPAC Commission on Molecular Structure and Spectroscopy, "Tables of Wavenumbers for the Calibration of Infrared Spectrometers", 2nd ed.; Cole, A. R. H., compiler; Pergamon Press: Oxford, 1977.

Contribution from the Department of Chemistry,
Faculty of Science, Hokkaido University, Sapporo 060, Japan

Clay Column Chromatography: Partial Resolution of Metal(III) Tris(acetylacetonate) on a Δ-Nickel(II) Tris(1,10-phenanthroline)-Montmorillonite Column

AKIHIKO YAMAGISHI

Received October 20, 1981

M$^{\mathrm{III}}$(acac)$_3$ (M = Co, Cr, Ru; acac = acetylacetonato) was partially resolved on a sodium-montmorillonite column, in which the whole cation-exchange site had been replaced by Δ-[Ni(phen)$_3$]$^{2+}$ (phen = 1,10-phenanthroline) stoichiometrically. The efficiency of resolution was outstanding in comparison with that of previously known methods, although the present column was only 2.5 cm in length. The mechanisms for the chirality recognition were discussed on the basis of molecular stacking between Δ-[Ni(phen)$_3$]$^{2+}$ and M$^{\mathrm{III}}$(acac)$_3$ in the interlamellar space.

A clay adsorbs an inorganic metal ion at its cation-exchange sites. It is believed that the site is usually generated by replacing an Al^{3+} ion in the alumina sheet with a divalent ion like Mg^{2+} or Fe^{2+}.[1] Since there exists no structural asymmetry around such a cation-binding site, a clay cannot discriminate a chiral compound intrinsically. Very recently, however, the present author has revealed that a metal complex with bulky ligands occupies the interlamellar space of clay in a rigorously stereoregular manner.[2,3] For example, when [Fe(phen)$_3$]$^{2+}$ (phen = 1,10-phenanthroline) was adsorbed on a colloidally dispersed sodium-montmorillonite, the complex tends to occupy a site as a racemic pair rather than as a single enantiomer.[3] Consequently, a solution containing Δ and Λ isomers in unequal amounts improves its optical purity, because the excessive racemate is eliminated as a clay-metal chelate adduct.[3] Another consequence of such racemic adsorption is that, when a clay has been modified by an enantiomer of one kind, it becomes stereoselective toward the adsorption of a complex of another kind.[4] For example, the adsorption rate of Λ-[Fe(phen)$_3$]$^{2+}$ on a Δ-[Ni(phen)$_3$]$^{2+}$-montmorillonite surface was 4 times faster than that of Δ-[Fe(phen)$_3$]$^{2+}$, because the former was a more preferable partner with Δ-[Ni(phen)$_3$]$^{2+}$ than the latter.

As the extension of the above findings, we investigated the chromatographic resolution on a column of a clay-chiral metal chelate complex. As a result, it is shown here that metal tris(acetylacetonate) has been efficiently resolved on a Δ-[Ni(phen)$_3$]$^{2+}$-montmorillonite column.

Experimental Section

Materials. Co(acac)$_3$, Cr(acac)$_3$, Ru(acac)$_3$, and Rh(acac)$_3$ were prepared according to the literature.[5] The compounds were identified from the electronic spectra. Sodium-montmorillonite (denoted by Na$^+$-M$^-$, M$^-$ being a cation-exchange site) was purchased from Kunimine Industrial Co. (Tokyo, Japan). The material contained 1 molar equiv of cation-exchange site/870 g.

Preparation of a Column. An aqueous solution of Δ-[Ni(phen)$_3$]Cl$_2$ (4 × 10^{-3} mol) was added at 2 °C into a solution of a colloidally dispersed Na$^+$-M$^-$ (7.0 g; 8.0 × 10^{-3} mol in terms of cation-exchange site) with stirring. The mixture was centrifuged to separate a clay-metal chelate adduct. The precipitate was washed with methanol several times and dried under vacuum for 2 days. The solid was ground into a fine powder (~9 g). A slurry of 1-2 g of solid (Δ-[Ni(phen)$_3$]$^{2+}$-2M$^-$) in water was poured into glass tubing to form a 2-4-cm column of 1.5-cm o.d. As a pretreatment, water was eluted at the flow rate of 0.2-0.3 mL s^{-1}. After elution with 10-15 mL of

---

(1) Theng, B. K. G. "The Chemistry of Clay-Organic Reactions"; Wiley: New York, 1974; Chapter 1.

(2) Yamagishi, A.; Soma, M. *J. Chem. Soc., Chem. Commun.* **1981**, 539.

(3) Yamagishi, A.; Soma, M. *J. Am. Chem. Soc.* **1981**, *103*, 4640.

(4) Yamagishi, A. *J. Chem. Soc., Chem. Commun.* **1981**, 1128.

(5) Fay, R. C.; Girgis, A. Y.; Klabunde, U. *J. Am. Chem. Soc.* **1970**, *92*, 7056 and references therein.

0020-1669/82/1321-3393$01.25/0